IEEE Access
Multidisciplinary | Rapid Review | Open Access Journal

Received 21 March 2023, accepted 25 April 2023, date of publication 28 April 2023, date of current version 9 May 2023.

Digital Object Identifier 10.1109/ACCESS.2023.3271357

RESEARCH ARTICLE

Multilayer Dry Film Photoresist Fabrication of a Robust >100 GHz Gap Waveguide Slot Array Antenna

SADIA FARJANA[1], ESPERANZA ALFONSO[2], PER LUNDGREN[1], VESSEN VASSILEV[1], PETER ENOKSSON[3], (Member, IEEE), AND ASHRAF UZ ZAMAN[4], (Senior Member, IEEE)

[1]Department of Microtechnology and Nanoscience, Chalmers University of Technology, 412 96 Gothenburg, Sweden
[2]Gapwaves AB, 412 63 Gothenburg, Sweden
[3]Enoaviatech AB, 112 26 Stockholm, Sweden
[4]Department of Electrical Engineering, Chalmers University of Technology, 412 96 Gothenburg, Sweden

Corresponding author: Sadia Farjana (farjana@chalmers.se)

This work was supported by Adlerbertska Forskningsstiftelsen Fund and FORWARD project funded by Strategic vehicle research and innovation program (FFI) 2018-02707.

ABSTRACT This article presents the first use of a multilayer dry film photoresist to fabricate a slot array antenna by micromachining. The proposed fabrication process demonstrates a straightforward and fast method of realizing antenna structures and delicate features with very high accuracy above 100 GHz. The slot array antenna design is based on gap waveguide technology. The designed antenna consists of two layers: a slot layer and a feed layer with a transition to measuring waveguide. The antenna contains structures that require a multiple level dry film fabrication process with thicknesses ranging from 80 μm to 400 μm with $\pm$10 μm tolerance. The fabricated antenna shows good accuracy. To make the fabricated antenna layers conductive, the fabricated polymer antenna was coated with Ti and Au. The input reflection coefficient was measured to be below – 11 dB over a 10% bandwidth from 136-148 GHz, and the antenna gain was measured to be 11.4 dBi at 142 GHz, both of which are in fair agreement with simulations. A thermal cycling test has been conducted on the fabricated antenna and the results show insignificant degradation at least up to 300 cycles in the temperature range -50 °C to 135 °C which is the typical temperature gradient range for many practical outdoor wireless applications.

INDEX TERMS Dry film photoresist, gap waveguide technology, microfabrication, micromachined millimeter wave antenna, slot array, thermal reliability.

I. INTRODUCTION

The terahertz (THz) (0.1-10 THz) frequency band is becoming the useful frequency band for future wireless systems due to the availability of large continuous bandwidth [1], [2] and it will be used in a wide range of applications from high data rate telecommunication and imaging to biomedicine [3], [4], [5], [6]. To facilitate the utilization of these benefits, work needs to be done on the development of low cost and high-performance passive components such as transmission lines, antennas, and filters. Above 100 GHz, passive waveguide components experience a big gap in available technologies in terms of combining performance, fabrication complexity, and cost. As soon as we move towards frequencies higher than 100 GHz, the dimensions of the passive components become so small that for conventional machine-based methods those dimensions are very challenging to manufacture with sufficient accuracy. Also, conventional CNC milling based serial manufacturing is inherently very time-consuming and becomes very costly.

Several micromachining techniques have proven themselves useful for fabricating passive waveguide components operating above 100 GHz: silicon (Si) micromachining [7], [8], SU-8 photoresist based micromachine technique [9], [10], and LIGA (Lithography, Electroplating, and Molding) [11], [12]. One general issue for micromachine-based

The associate editor coordinating the review of this manuscript and approving it for publication was Chinmoy Saha.

methods is that they typically require time-consuming processing steps. Apart from this, planarity requirements, vertical sidewall issues, edge bead problems, stress-related bending, and the need for sophisticated fabrication facilities make the existing micromachine processes both technically challenging and costly [13].

Recently, dry film photoresist has been used to fabricate passive waveguide components operating above 100 GHz. The first dry film-based waveguide component has been demonstrated with high fabrication accuracy, which together with the performance of the fabricated chip indicated that the dry film-based process can be a suitable method to manufacture high-frequency passive components where the tolerances are crucial [14]. In contrast to spin coating, dry films are thermally laminated onto a substrate or a carrier, and the lamination process requires very short time, offering significant benefits compared to other materials commonly used in microfabrication. Still, multiple-level fabrication by dry film photoresist can be challenging in terms of delamination of separately patterned layers, misalignment caused during layer patterning, due to limited transparency of thick photoresist, and nonvertical side walls caused by overexposure of the previously laminated layer. Generally, accurate layer-to-layer alignment is critical and is realized by inserting alignment features on each mask layer and orienting each photomask to align with markers on previous layers. Using SUEX dry film photoresist, alignment with the previously laminated layer was not required [15], [16]. It has been demonstrated by other groups that to obtain multilayer structure by dry film photoresist, the first layer needs to be fully developed, making the pattern visible, before patterning the second layer, or they have chosen a very long post-exposure bake (PEB) time [17], [18]. However, developing the patterned structure for each layer separately comes with a directly increased time consumption. In this article, we demonstrate that by proper optimization of the exposure dose and PEB time, SUEX dry film photoresist (DJ MICROLAMINATES Inc.) can be used for multilayer fabrication. The demonstrated micromachined slot array antenna is based on gap waveguide (GW) technology.

GW technology has proven itself a promising candidate for waveguide components operating at mmWave and THz frequency as the tradeoff between the device performance in terms of gain, working bandwidth, efficiency to the size of the device, and manufacturing complexities are quite competitive; GW offers benefits of planar geometry, high device performance without suffering from dielectric loss, and low complexity manufacturing due to the non-contact nature of this waveguide. By maintaining an air gap less than $\lambda/4$ between the metal blocks, wave-propagation in an unwanted direction is prohibited, and hence the local waves follow the specific guiding structures such as strips, ridges, or grooves which are embedded within the Perfect Electric Conductor (PEC)- Perfect Magnetic Conductor (PMC) parallel-plate configuration [19], [20]. GW based passive components such as antenna, and filter have been demonstrated both at low and high frequency up to 100 GHz over the last few years [21], [22]. Different types of transitions from GW to rectangular waveguide (WG), microstrip line, and coplanar WG have also been proposed and demonstrated and can be used for the integration of active and passive devices [15], [23], [24], [25], [26].

The antenna fabrication requires a multilayer dry film fabrication process with thicknesses ranging from 80 μm to 400 μm. A two-port antenna with two identical ridge gap waveguide (RGW) end-fed linear slot arrays was designed to study the similarity between ports and hence the robustness of the fabrication method. The fabricated antenna operates in the D-band. The proposed antenna has two functional layers, the slot layer, and the feed layer. The feed layer contains structures of different heights, thus requiring multilayer fabrication. The presented fabrication process not only provides a low-cost solution but furthermore indicates that dry film photoresist is a suitable material where multiple level fabrication is required with high accuracy. The measurement results for the antenna show good agreement with simulations. Additionally, a reliability test was performed by subjecting the device to thermal cycling. As the thermal expansion coefficients differ between the polymer and the deposited conductive layer, the material combination could potentially induce degradation or failure in applications where temperature variations occur. The fabricated antenna did however show no signs of degradation after a thermal cycling test of 300 cycles in the temperature range −55 °C to 135 °C. This opens new doors for a wide range of applications for devices fabricated using this novel fabrication technology.

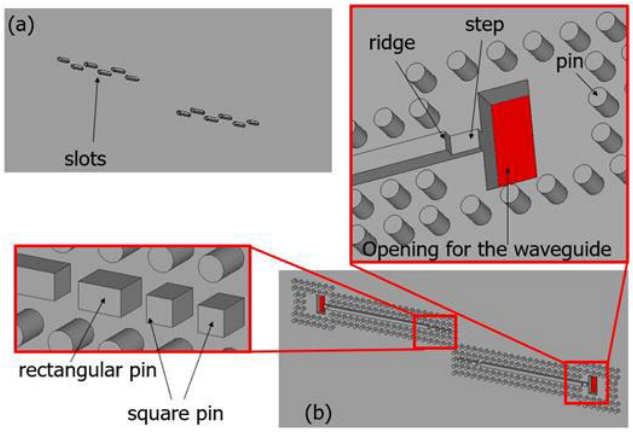

FIGURE 1. Geometrical design of the proposed slot array antenna in CST Microwave studio, (a) the slot layer, (b) the feed layer and a close view of the ridge, pin, and step that forms the transition from ridge gap waveguide to WR6.5.

II. GEOMETRY AND DESIGN OF THE PROPOSED ANTENNA

A simple ridge gap waveguide (RGW) slot array antenna has been designed to validate the dry film-based fabrication

process. The slot layer consists of two columns of six longitudinal slots each, both of which are fed by a RGW that has been terminated with an open circuit to generate a standing wave inside. The two columns are fed independently, and therefore the antenna has two WR6.5 rectangular waveguide input ports, as shown in Fig.1.

The RGW end-fed linear slot array is a typical design of longitudinal slots located with an offset from the waveguide center-axis at both sides alternatingly, and where the spacing between slots is approximately λ/2. The dimensions of the slots (width and length) and the offset from the waveguide center-axis and distance between them are optimized for impedance matching and maximum radiated gain using the commercial software CST Microwave Studio. The slot thickness is chosen to be 0.4 mm for sufficient stiffness and planarity of the slot layer. The ridge gap waveguide dimensions (ridge, pins and air gap) are chosen to have only one transverse-electric mode (TEM) propagating within the 110 GHz to 170 GHz band. Finally, to be able to measure the antenna using a standard WR6.5 flange, a D-band transition from ridge gap waveguide to WR6.5 rectangular waveguide consisting of a step in the ridge was designed. The dimensions, including pins, ridge, step, and slots are detailed in Table 1. Slot lengths, offsets, and distance between slots are different for each slot, and not stated here for brevity. The simulation results shown below correspond to one of the end-fed linear slot arrays. The impedance matching is revealed by the resulting S_{11} parameter displayed in Fig. 2b, and this is below -12 dB within a wide frequency band, from 136 to 148 GHz, which is the band of interest. During the simulation we have chosen gold as material and total simulated insertion loss including the flange transition and the feeding ridge was 0.3 dB.

TABLE 1. Dimensions of the antenna geometry: ridge, pins, step, and slots.

Parameter	Description	Value
P_h	Pin height	380 µm
A	Pin diameter	275 µm
R_w	Ridge width	275 µm
R_l	Ridge length	8.74 mm
R_h	Ridge height	300 µm
S_h	Step height	120 µm
S_l	Step length	400 µm
A_s	Area of square pin	275 × 275 µm^2
A_r	Area of rectangular pin	456 × 275 µm^2
S_w	Slot width	302 µm
S_t	Slot thickness	400 µm

At 140 GHz even a microscopic air gap between the antenna port and the measurement flange introduces significant leakage, which reduces the reliability of the measurement. To minimize leakage, a gap waveguide flange is introduced on the back side of the antenna, as can be seen in Fig. 2a. The pin-flange adapter was previously used to avoid leakage at the interface of two waveguides [27]. The introduction of the flange implies a slight change of the total reflection coefficient. A comparison of the S_{11} with and without a gap waveguide flange is shown in Fig. 2b, where it can be noted that S_{11} is still below -12 dB over the band of interest. In the simulation, an airgap of 25 μm has been used between the gap waveguide flange and the antenna excitation port.

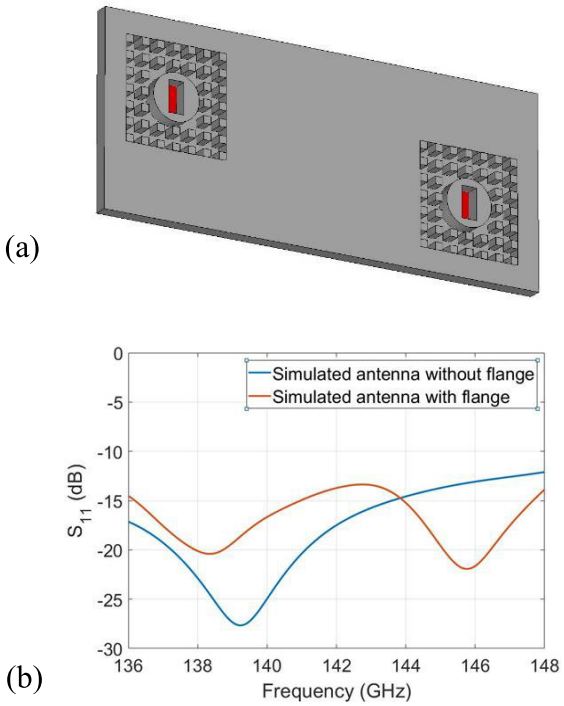

FIGURE 2. (a) Back of the antenna with inserted gap waveguide flanges; (b) Simulated S_{11} of the slot array with and without gap waveguide flange structure.

The presented ridge gap waveguide has been designed based on the zero-gap waveguide concept and has already been demonstrated [28]. However, considering the fabrication tolerance, the air gap between the feed layer and the slot layer has been maintained 10 μm, that is <λ/4 at 140 GHz, during the simulation. Since a variation of the air gap will introduce changes in the propagation characteristics of the RGW, i.e., characteristic impedance and propagation constant, it may affect the antenna performance and especially the impedance matching. Fig. 3 shows the impedance matching for air gaps from 0 μm to 20 μm, where S_{11} remains below −10 dB within the band.

III. FABRICATION PROCESS

The slot and the feed layers have been fabricated separately and the optimization of the fabrication steps has been done based on the geometry of the respective structures.

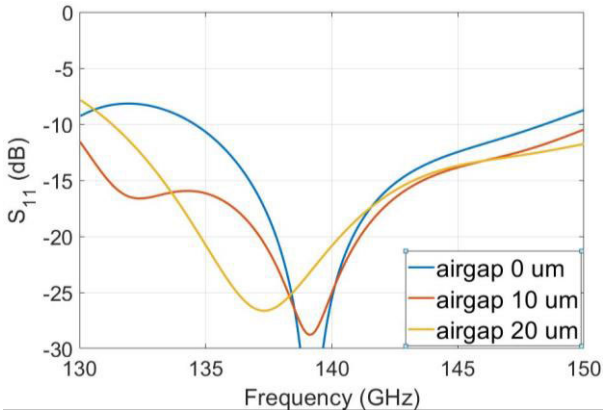

FIGURE 3. Simulated impedance matching (S_{11}) of the RGW end-fed linear slot array antenna for several air gaps from 0 to 20 μm.

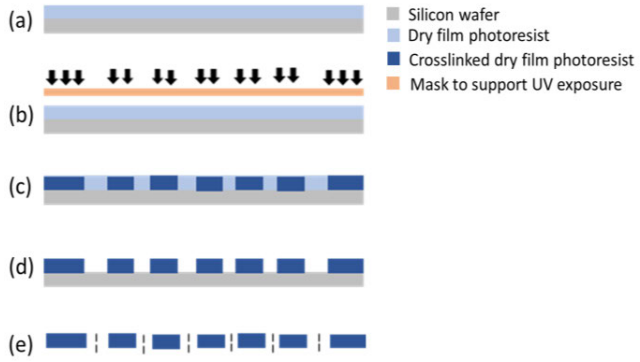

FIGURE 4. Schematic of the complete slot layer fabrication process.

The SUEX dry film is a negative-tone photoresist sandwiched between two polyester (PET) films. The general fabrication steps are lamination of the dry film on a substrate, UV exposure of the photoresist, post-exposure bake, development of the photoresist, and removal of the photoresist from the substrate. A laminator (PRO SERIESTM 3600) has been used to laminate the dry films on a silicon (Si) wafer substrate. The laminator temperature has been set to 65 °C and the speed of the lamination has been maintained at 5 mm/sec. Dry film photoresists come in predefined thicknesses. Multiple dry film sheets can be laminated to achieve the required thickness. The detailed lamination process is explained below.

A. FABRICATION OF THE SLOT LAYER

The fabrication of the slot layer is simple as it requires only a single fabrication process. The thickness of the slot layer in our design was 400 μm. A Si wafer was used as a substrate and a 400 μm thick SUEX film was laminated on the wafer followed by UV exposure with a mask to obtain the patterns of the intended slot layer. The exposure energy of 9000 mJ/cm^2 has been optimized to crosslink the 400 μm thick SUEX film. Two steps of post-exposure bake (PEB) have been carried out, by starting the baking at 65 °C for 10 min followed by a bake at 95 °C for 1 hr.

The photoresist development employed two different baths using the developer mr-DEV 600. The wafer has been kept in the first bath for 30 min without any agitation. The wafer was subsequently moved to a fresh bath and kept there for another 30 min with mild agitation. After that, the fabricated piece has been rinsed with isopropyl alcohol (IPA) and kept in an IPA bath for 5 min. It was then subjected to a drying step at 100 °C for 5 min on the hot plate followed by hard baking at 120 °C for 10 min and 150 °C for another 10 mins.

To make the surface conductive, 50 nm of titanium (Ti) and 200 nm of gold (Au) have been deposited by sputtering, followed by electroplating of 1.4 μm of Au. Fig. 4 shows the schematic of the complete fabrication process.

B. FABRICATION OF THE FEED LAYER

The feed layer consists of a base layer that contains the opening for the waveguide, a ridge with a step, and pins. To define all the structures, multiple-layer fabrication has been needed and the fabrication process has been tuned to obtain the structures. Fig. 5 shows the schematic of the complete multilayer fabrication process.

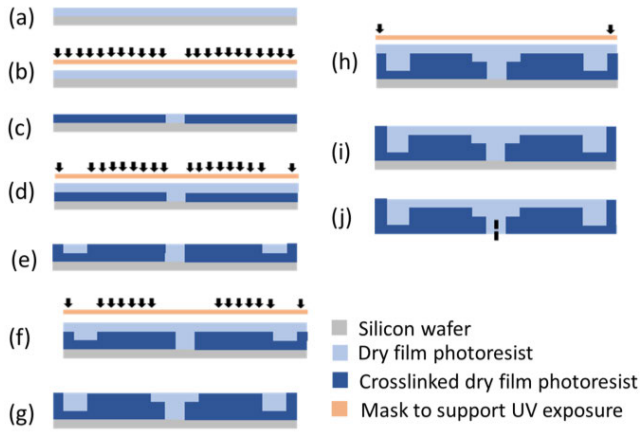

FIGURE 5. Schematic of the complete feed layer fabrication process.

To fabricate the 400 μm thick base layer two 200 μm thick SUEX dry film photoresists have been used, considering the availability of dry film sheets in the lab. A Si wafer was used as a carrier. A post lamination bake (PLB) at 65 °C for 1 min 30 sec has been done to assure the adhesion between the laminated sheets. The laminated sheets were then going through a UV exposure with the exposure energy of 9000 mJ/cm^2, with a photomask defining the opening for the waveguide followed by a two steps PEB similar as the slot layer fabrication.

The next layer fabrication was designed to define the step in the ridge and partial height of the pins. To define the 120 μm thick step in the ridge we used two dry film sheets of thicknesses 100 μm and 20 μm respectively. The 100 μm thick SUEX film has been laminated on the patterned base layer followed by a PLB of 1 min. The 20 μm thick SUEX film was laminated on the 100 μm SUEX film and went through a 30 sec long PLB. The laminated films were then UV

exposed with a mask defining the step, ridge, and pins with 3000 mJ/cm^2 exposure energy followed by a PEB at 95 °C for 30 min. To define the remaining height of the ridge and partial height of the pins one SUEX film of 100 μm and two SUEX films of 40 μm have been laminated on the previously patterned layer followed by a PLB of 1 min, 30 sec, and 30 sec respectively. The laminated SUEX film was then UV exposed with 4000 mJ/cm^2 exposure energy with a mask defining the ridge and the pins. A PEB at 95 °C for 30 min was performed later. To define the remaining height of the pins two SUEX films of 40 μm were laminated to the previously patterned layer. After lamination of each sheet, a PLB of 30 sec has been performed to assure the adhesion between the laminated layers to the patterned layer. The laminated sheets were then UV exposed with a mask defining the pins with 1800 mJ/cm^2 exposure energy and a PEB of 30 min at 95 °C was performed.

The photoresist then went through development, hard baking, and conductive layer deposition process, similar as the slot layer fabrication process and described in section III-A.

IV. RESULTS AND DISCUSSION

In this section, we present the fabrication result, and measurement results, together with discussions of the results.

A. FABRICATION RESULTS

Fig. 6. shows the fabricated chips. The achieved slot layer thickness was 404 ± 2 μm, the height of the step in the ridge was 123 ± 2 μm, the height of the ridge was 304 ± 2 μm, and pins were 385 ± 2 μm. The surface roughness of the fabricated chip has been measured as it has a significant effect on the performance of the device. The measured surface roughness of the fabricated chip was 8.7 ± 0.5 nm. Fig 7. shows SEM images of the fabricated antenna.

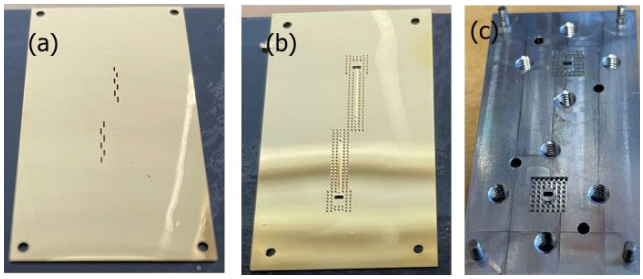

FIGURE 6. Fabricated antenna. (a) slot layer, (b) feed layer, (c) supporting bottom plate with WR-6.5 opening and gap waveguide pin flange structure.

SUEX films are not completely transparent, making alignment of multiple layers challenging. The optimization of the exposure does and the PEB time have been done to obtain sufficient visibility of the patterned alignment mark in conjunction with achieving straight sidewalls.

B. MEASURMENT RESULTS

The measurement was done using a Keysight PNA N5242A and VDI D-band extender module having a WR-6.5

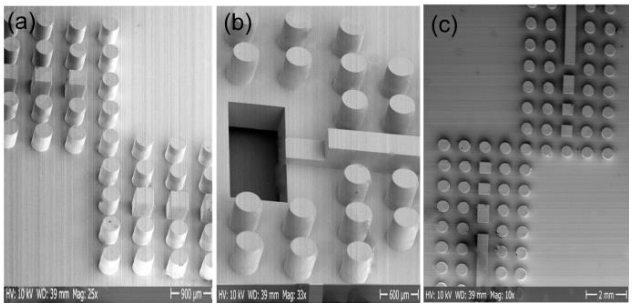

FIGURE 7. SEM images of the fabricated antenna. (a) circular, and square pins, (b) opening for the waveguide on the base plate of the feed layer and step in the ridge (c) image showing partial feed layer containing ridge, square pins, rectangular pins, and circular pins.

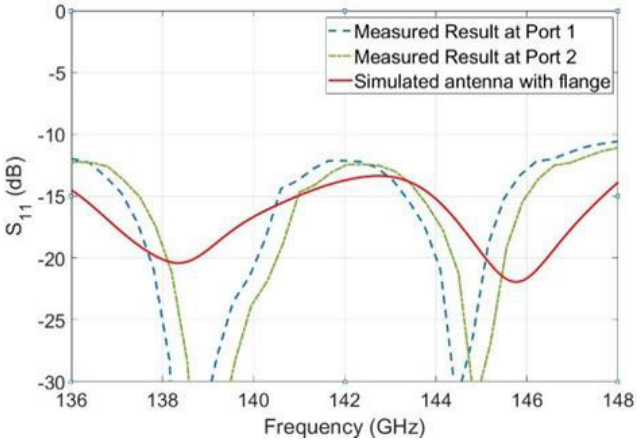

FIGURE 8. Simulated and measured S_{11} of the fabricated antenna.

waveguide interface. A milled metal piece with a gap waveguide pin flange structure was used to connect the flange and the fabricated pieces as shown in Fig 6c. A milled rim was used to maintain 10 μm airgap between the feed layer and the slot layer. Four alignment pins were used to align the fabricated pieces as shown in Fig 6c.

Fig 8. presents the S_{11} measurement results of the fabricated antenna. Both ports of the antenna were measured to evaluate the robustness of the fabrication method and the measurements are compared to simulation. Good agreement with the simulation result is observed and the measured S_{11} is below −10 dB over the band of interest.

The radiation pattern and the gain of the linear array antenna were measured in an anechoic chamber maintaining the far-field measurement condition. The simulated and measured radiation patterns are presented in Fig 9. The radiation patterns have been presented at 136 GHz, 142 GHz, and 148 GHz. The H-plane radiation patterns have a 3-dB beamwidth of 7°, 6.5°, and 5°, respectively. There exist some discrepancies between the simulated and measured patterns. However, the deviation between simulated and measured radiation patterns is rather low and within an acceptable level.

The measured total gain is about 11.4 dBi at 142 GHz and about 11 dBi over the band of interest from 136-148 GHz

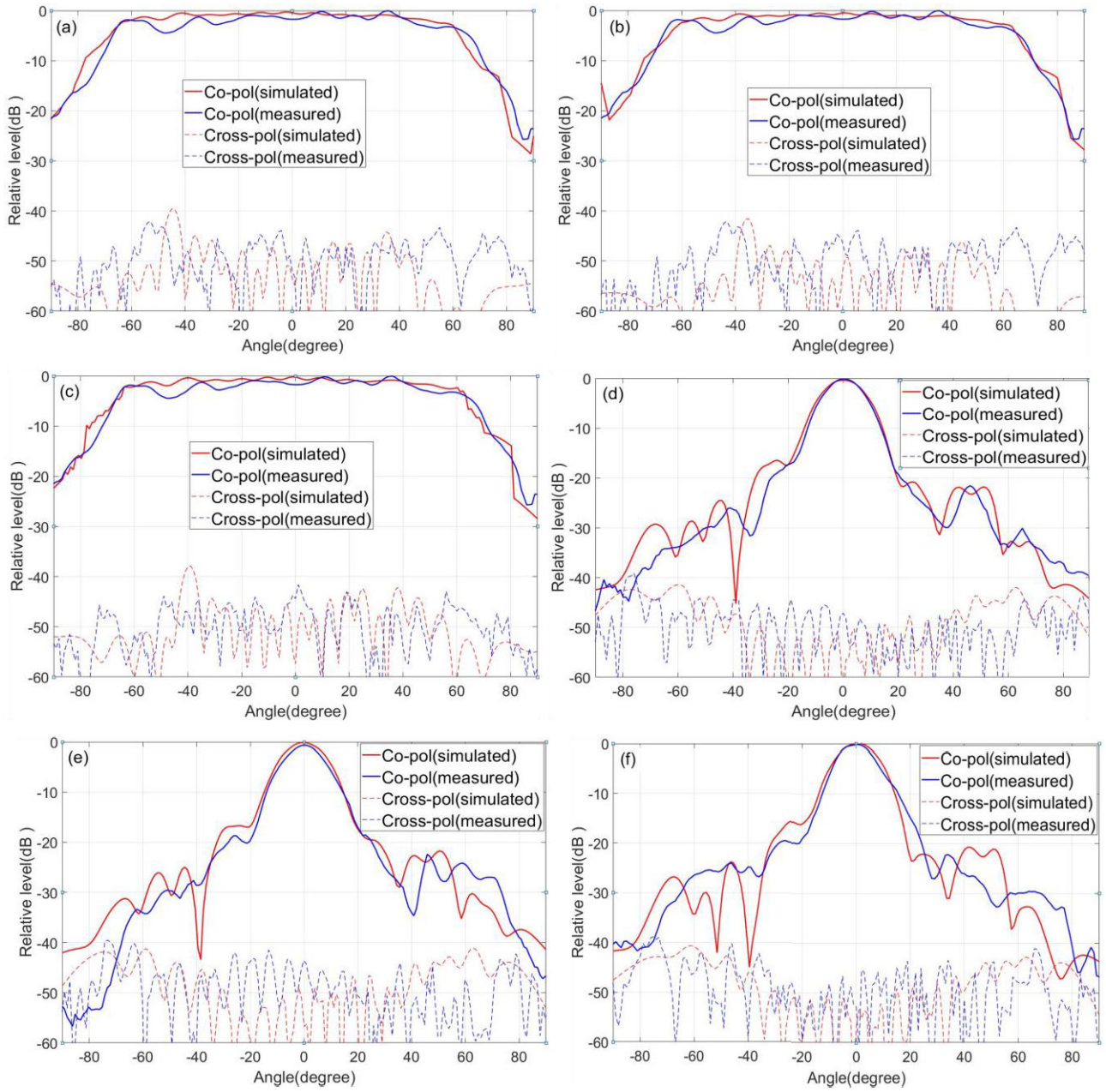

FIGURE 9. Comparison between simulated and measured radiation patterns of the proposed antenna. (a) E-plane at 136 GHZ, (b) E-plane at 142 GHZ, (c) E-plane at 148 GHZ, (d) H-plane at 136 GHZ, (e) H-plane at 142 GHZ, (f) H-plane at 148 GHZ.

and the gain vs frequency plot is presented in Fig 10. The total efficiency of the antenna is 95% and can be seen in Fig 10. A D-band horn antenna with known gain value was used as a reference antenna for gain measurement. The measured gain is about 0.6-0.4 dB less than the simulated gain. A comparison between the proposed antenna and other linear array antennas is given in Table 2. This can be attributed to slight airgap variations, insertion loss and micrometer scale misalignment when mounting the different layers of the antenna. The gain measurement plot also presents the gain of the antenna after performing 300 cycles of thermal cycling. Details of the thermal cycling test will be mentioned in section IV-C.

C. RELIABILITY TEST

Reliability investigation of any material is essential for commercial applications. Thermal stress induced during temperature cycling can cause a significant effect due to a large coefficient of thermal expansion (CTE) mismatch between the polymer (∼50 ppm/°C) [33] and the deposited conductive layer AU (∼14 ppm/°C). The temperature range of the test was −50 to 135 °C with a ramp-up time of 10 min and

TABLE 2. Comparison of performance between the proposed antenna and other antennas.

Ref	Tech	Freq (GHz)	No. of elements	Gain (dB)	*Eff.%
[29]	PCB	60-90	4×1	10	67
[30]	Patch array	259-291	4×1	5.2	-
[31]	SIW	70-90	4×1	6	43
[32]	GW	95-108	4×1	10.4	86
This work	GW	136-148	6×1	11.4	95

*Eff. = Efficiency at center frequency.

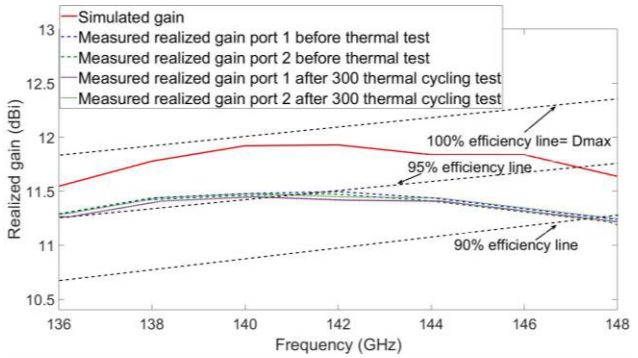

FIGURE 10. Simulated and measured realized gain of the antenna before and after the thermal cycling test.

30-min dwell time. The reflection coefficient and the surface roughness of the antenna have been measured after 75, 150, and 300 thermal cycles.

The surface roughness was measured by an atomic force microscope (AFM) after each round of thermal cycling test. The measured surface roughness of the fabricated chip was 8.7 ± 0.5 nm before any thermal cycling. The surface roughness increased after thermal cycling and was measured to 28.2 ± 2 nm after 75 thermal cycles, 32.4 ± 2 nm after 150 thermal cycles, and 64.5 ± 4 nm after 300 thermal cycles. The surface roughness of the fabricated chip has increased by about 55 nm after 300 thermal cycles, but the total surface roughness is still much smaller than the skin depth (200 nm) at the operating frequency. It is therefore expected to have a negligible effect on the electrical performance of the antenna. Different groups have observed a similar effect on deposited Au, where the surface roughness increases with increased temperature [34], [35]

Fig 11 shows the S_{11} measurement results after 75, 150, and 300 thermal cycles. The measured S_{11} is below -11 dB within the band of interest even after conducting the thermal cycling tests. The slight mismatch among the measurement

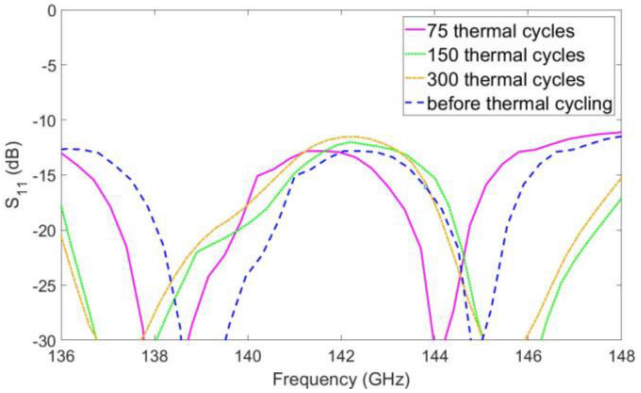

FIGURE 11. Simulated and measured S_{11} of the fabricated antenna before and after the thermal cycling test.

results could have been induced during mounting the fabricated pieces with the milled supporting piece, and/or during mounting of the antenna to the waveguide flange. The airgap variations and rotational error introduced between milled and micromachined pieces can be slightly different in each round of measurement. To check the effect of rotational error and alignment error between the layers we introduced $\pm 1°$ rotational misalignment and ± 10 μm misalignment between the fabricated layers in the simulation. To avoid complexity, we maintained 10 μm constant airgap during this simulated tolerance check. The simulation results showed at least 1-1.5 GHz frequency shift in the reflection coefficient after introducing those alignment errors, matching the observed behavior in the measurements. Hence, the reflection coefficient measurement results indicate that the fabricated antenna can perform similarly before and after the thermal cycling tests. The gain measurement result presented in Fig 10 indicate that the antenna can operate at least after 300 thermal cycles.

V. CONCLUSION

A fabrication technique based on SUEX dry film photoresist has been demonstrated for the fabrication of a robust gap waveguide slot array antenna comprising features of several hundred micrometers with a feature fidelity on the single micrometer level and below 10 nm surface roughness. The fabricated antenna demonstrates the successful employment of a multiple level dry film fabrication process with thicknesses ranging from 80 μm to 400 μm. The overall radiation performance of the antenna elements consisting of two Au-coated polymer layers is satisfactory. The input reflection coefficient was measured to be below -11 dB over a 10 % bandwidth from 136-148 GHz, and the antenna gain was measured to be 11.4 dBi at 142 GHz, both of which are results in fair agreement with fullwave simulations. Also, in a thermal cycling test of up to 300 cycles, we have not observed any significant performance degradation for the fabricated antenna. The results from the thermal cycling indicate that, along with delivering waveguide components with high dimensional accuracy, the proposed fabrication

method can be used to fabricate robust waveguide components with reliable operation in environments with large temperature variations.

ACKNOWLEDGMENT

The authors would like to thank John Halonen of the Nanofabrication Laboratory for his help and support during developing the fabrication process and thankful to the project partners from Gapwaves, Veoneer, and CEVT, for their constructive feedback.

REFERENCES

[1] D. Lockie and D. Peck, "High-data-rate millimeter-wave radios," *IEEE Microw. Mag.*, vol. 10, no. 5, pp. 75–83, Aug. 2009.

[2] D. M. Mittleman, "Perspective: Terahertz science and technology," *J. Appl. Phys.*, vol. 122, no. 23, Dec. 2017, Art. no. 230901.

[3] K. Fan, Z.-C. Hao, Q. Yuan, and W. Hong, "Development of a high gain 325–500 GHz antenna using quasi-planar reflectors," *IEEE Trans. Antennas Propag.*, vol. 65, no. 7, pp. 3384–3391, Jul. 2017.

[4] R. Knipper, "THz absorption in fabric and its impact on body scanning for security application," *IEEE Trans. terahertz Sci. Technol.*, vol. 5, no. 6, pp. 999–1004, May 2015.

[5] B. Cheng, "340-GHz 3-D imaging radar with 4Tx-16Rx MIMO array," *IEEE Trans. Terahertz Sci. Technol.*, vol. 8, no. 5, pp. 509–519, May 2018.

[6] H.-J. Song and T. Nagatsuma, "Present and future of terahertz communications," *IEEE Trans. Terahertz Sci. Technol.*, vol. 1, no. 1, pp. 256–263, Sep. 2011.

[7] A. Gomez-Torrent, "A low-profile and high-gain frequency beam steering subterahertz antenna enabled by silicon micromachining," *IEEE Trans. Antennas Propag.*, vol. 68, no. 2, pp. 672–682, Feb. 2020.

[8] K. Tekkouk, "Corporate-feed slotted waveguide array antenna in the 350-GHz band by silicon process," *IEEE Trans. Antennas Propag.*, vol. 65, no. 1, pp. 217–225, Dec. 2017.

[9] C. Guo, Y. Dhayalan, X. Shang, J. Powell, M. J. Lancaster, J. Xu, Y. Wang, H. Wang, B. Alderman, and P. G. Huggard, "A 135–150-GHz frequency tripler using SU-8 micromachined WR-5 waveguides," *IEEE Trans. Microw. Theory Techn.*, vol. 68, no. 3, pp. 1035–1044, Mar. 2020.

[10] H. Yang, "WR-3 waveguide bandpass filters fabricated using high precision CNC machining and SU-8 photoresist technology," *IEEE Trans. Terahertz Sci. Technol.*, vol. 8, no. 1, pp. 100–107, Nov. 2018.

[11] O. V. Makarova, R. Divan, J. Tucek, K. Kreischer, and C.-M. Tang, "Fabrication of solid copper two-level waveguide circuits for a THz radar system by UV lithography," in *Proc. IEEE Int. Vac. Electron. Conf. (IVEC)*, Apr. 2016, pp. 1–5.

[12] Y. Li, "Terahertz rectangular waveguides by UV-LIGA with megasonic agitation," *Micromachines*, vol. 13, pp. 456–564, Dec. 2022, doi: 10.3390/mi13101601.

[13] G. Chattopadhyay, T. J. Reck, C. Jung-Kubiak, J. V. Siles, C. Lee, R. Lin, and I. Mehdi, "Silicon micromachining for terahertz component development," in *IEEE MTT-S Int. Microw. Symp. Dig.*, Dec. 2013, pp. 123–142.

[14] S. Farjana, M. Ghaderi, S. Rahiminejad, S. Haasl, and P. Enoksson, "Dry film photoresist-based microfabrication: A new method to fabricate millimeter-wave waveguide components," *Micromachines*, vol. 12, no. 3, p. 260, Mar. 2021.

[15] S. Farjana, M. Ghaderi, A. U. Zaman, S. Rahiminejad, P. Lundgren, and P. Enoksson, "Low-loss gap waveguide transmission line and transitions at 220–320 GHz using dry film micromachining," *IEEE Trans. Compon., Packag., Manuf. Technol.*, vol. 11, no. 11, pp. 2012–2021, Nov. 2021.

[16] S. Farjana, A. U. Zaman, P. Lundgren, and P. Enoksson, "Micromachined wideband ridge gap waveguide power divider at 220–325 GHz," *IEEE Access*, vol. 10, pp. 27432–27439, 2022.

[17] V. Mulloni, A. Capuano, A. Adami, A. Quaranta, and L. Lorenzelli, "A dry film technology for the manufacturing of 3-D multi-layered microstructures and buried channels for lab-on-chip," *Microsyst. Technol.*, vol. 25, no. 8, pp. 3219–3233, Aug. 2019.

[18] N. E. Koucherian, S. Yan, and E. E. Hui, "Fabrication of multilayer molds by dry film photoresist," *Micromachines*, vol. 13, no. 10, p. 1583, Sep. 2022, doi: 10.3390/mi13101583.

[19] P. Kildal, "Three metamaterial-based gap waveguides between parallel metal plates for mm/submm waves," in *Proc. 3rd Eur. Conf. Antennas Propag.*, 2009, p p. 167–187.

[20] E. Rajo-Iglesias, M. Ferrando-Rocher, and A. U. Zaman, "Gap waveguide technology for millimeter-wave antenna systems," *IEEE Commun. Mag.*, vol. 56, no. 7, pp. 14–20, Jul. 2018.

[21] A. Vosoogh, "W-band low-profile monopulse slot array antenna based on gap waveguide corporate-feed network," *IEEE Trans. Antennas Propag.*, vol. 66, no. 12, pp. 6997–7009, Jul. 2018.

[22] M. Rezaee and A. U. Zaman, "Realisation of carved and iris groove gap waveguide filter and E-plane diplexer for V-band radio link application," *IET Microw., Antennas Propag.*, vol. 11, no. 15, pp. 2109–2115, Oct. 2017.

[23] C. Biurrun-Quel, J. Teniente, and C. del-Río, "Reduced loss and prevention of substrate modes with a novel coplanar waveguide based on gap waveguide technology," *Sensors*, vol. 23, no. 6, p. 2909, Mar. 2023.

[24] A. U. Zaman, V. Vassilev, H. Zirath, and N. Rorsman, "Novel low-loss millimeter-wave transition from waveguide-to-microstrip line suitable for MMIC integration and packaging," *IEEE Microw. Wireless Compon. Lett.*, vol. 27, no. 12, pp. 1098–1100, Dec. 2017.

[25] A. Hassona, V. Vassilev, A. U. Zaman, V. Belitsky, and H. Zirath, "Compact low-loss chip-to-waveguide and chip-to-chip packaging concept using EBG structures," *IEEE Microw. Wireless Compon. Lett.*, vol. 31, no. 1, pp. 9–12, Jan. 2021.

[26] Q. Ren, A. U. Zaman, J. Yang, V. Vassilev, and C. Bencivenni, "Novel integration techniques for gap waveguides and MMICs suitable for multilayer waveguide applications," *IEEE Trans. Microw. Theory Techn.*, vol. 70, no. 9, pp. 4120–4128, Sep. 2022.

[27] S. Rahiminejad, E. Pucci, S. Haasl, and P. Enoksson, "Micromachined contactless pin-flange adapter for robust high-frequency measurements," *J. Micromech. Microeng.*, vol. 24, no. 8, Aug. 2014, Art. no. 084004.

[28] A. Vosoogh, A. U. Zaman, V. Vassilev, and J. Yang, "Zero-gap waveguide: A parallel plate waveguide with flexible mechanical assembly for mm-wave antenna applications," *IEEE Trans. Compon., Packag., Manuf. Technol.*, vol. 8, no. 12, pp. 2052–2059, Dec. 2018.

[29] C. Vasanelli, T. Ruess, and C. Waldschmidt, "A 77-GHz cavity antenna array in PCB technology," in *Proc. IEEE 15th Medit. Microw. Symp. (MMS)*, Nov. 2015, pp. 1–8.

[30] B. Benakaprasad, A. Eblabla, X. Li, I. Thayne, D. J. Wallis, I. Guiney, C. Humphreys, and K. Elgaid, "Terahertz monolithic integrated circuits (TMICs) array antenna technology on GaN-on-low resistivity silicon substrates," in *Proc. 41st Int. Conf. Infr., Millim., Terahertz waves (IRMMW-THz)*, Sep. 2016, pp. 1–2.

[31] S. Cheng and H. H. Yousef Kratz, "79 GHz slot antennas based on substrate integrated waveguides (SIW) in a flexible printed circuit board," *IEEE Trans. Antennas Propag.*, vol. 57, no. 1, pp. 64–71, Dec. 2009.

[32] S. Rahiminejad, A. U. Zaman, S. Haasl, P.-S. Kildal, and P. Enoksson, "Demonstration of a micromachined planar distribution network in gap waveguide technology for a linear slot array antenna at 100 GHz," *J. Micromech. Microeng.*, vol. 26, no. 7, Jul. 2016, Art. no. 074001.

[33] *Product Data Sheet, SUEX Thick Dry Film Sheets (TDFS)*, Microlaminates, Jun. 2020.

[34] S. B. Dimitrijev, M. M. Raj-Vujasinovi, R. M. Jan-Hajneman, J. B. Bajat, V. K. Truji, and D. D. Trifunovi, "Temperature effect on decorative gold coatings obtained from electrolyte based on mercaptotriazole—Comparison with cyanide," *Int. J. Mater. Res.*, vol. 105, no. 3, pp. 272–281, Mar. 2014.

[35] H. Reddy, U. Guler, A. V. Kildishev, A. Boltasseva, and V. M. Shalaev, "Temperature-dependent optical properties of gold thin films," *Opt. Mater. Exp.*, vol. 6, pp. 2776–2802, Sep. 2016.

SADIA FARJANA was born in Bangladesh. She received the B.Sc. degree in electrical and electronics engineering and the M.Sc. degree from the Chittagong University of Engineering and Technology, Gothenburg, Sweden, where she is currently pursuing the Ph.D. degree. Her research interests include the field of micro and nanosystem technology and fabrication.

ESPERANZA ALFONSO received the M.Sc. and Ph.D. degrees in telecommunications engineering from Universidad Politécnica de Valencia (UPV), Valencia, Spain, in 2004 and 2011, respectively. From 2004 to 2010, she was a Research Assistant with Instituto de Telecomunicaciones y Aplicaciones Multimedia (ITeAM), UPV. From 2011 to 2013, she was a Postdoctoral Researcher in antenna systems with the Chalmers University of Technology, Gothenburg, Sweden, where she contributed to the development of passive microwave devices and millimeter-wave antennas in gap waveguide technology. Since 2013, she has been a Senior Antenna Engineer with Gapwaves AB, Gothenburg. Currently, her main experience is in antenna design in gap waveguide technology, with the focus on automotive applications. Her research interests include antennas and microwave engineering.

PER LUNDGREN received the Ph.D. degree from the Chalmers University of Technology, Sweden, in 1996. Since 2000, he has been an Associate Professor with the Chalmers University of Technology. His technical expertise is in the field of solid state electronics, where he focuses on integration challenges for novel nanostructures in electronics.

VESSEN VASSILEV received the M.Sc. degree in radio communications from Sofia Technical University, Sofia, Bulgaria, in 1995, the M.Sc. degree in digital communications from the Chalmers University of Technology, Gothenburg, Sweden, in 1998, and the Ph.D. degree from the Department of Radio and Space Science, Chalmers University of Technology, in 2003. From 1998 to 2008, he was involved in the development of cryogenic millimeter-wave receivers for applications in radio astronomy and space sciences. Instruments designed by him have been in operation at the Atacama Pathfinder Experiment (APEX) Telescope, Chile, and Onsala Space Observatory, Sweden. Since 2008, he has been with the Microwave Electronics Laboratory, Department of Microtechnology and Nanoscience, Chalmers University of Technology. His current research interest includes the development of millimeter-wavelength sensors based on monolithic microwave integrated circuit technologies.

PETER ENOKSSON (Member, IEEE) received the M.Sc. degree in engineering physics and the Ph.D. degree from the KTH Royal Institute of Technology, Stockholm, Sweden, in 1986 and 1997, respectively.

In 1997, he was an Assistant Professor first and then an Associate Professor with the KTH Royal Institute of Technology, in 2000. In 2001, he was a Professor of MEMS/MOEMS with the Chalmers University of Technology, Gothenburg, Sweden. From 2002 to 2004, he was the Vice Dean of the School of Electrical Engineering and the Head of the Solid State Electronics Laboratory, from 2003 to 2006. He was the Head of the Microsystem and Nanosystems Group, Department of Microtechnology and Nano Science, MC2. He is an initiator of spin-off companies. He has authored more than 300 research journals and conference papers and holds more than ten patents. His current research interests include energy storage, metamaterials, and MEMS/NEMS with other sciences in novel dedicated and advanced systems.

Dr. Enoksson was a recipient of the Innovation Cup. He is referee of several journals and an Editorial Board Member of the *Journal of Micromechanics and Microengineering*.

ASHRAF UZ ZAMAN (Senior Member, IEEE) was born in Chittagong, Bangladesh. He received the B.Sc. degree in electrical and electronics engineering from the Chittagong University of Engineering and Technology, Chittagong, and the M.Sc. and Ph.D. degrees from the Chalmers University of Technology, Gothenburg, Sweden, in 2007 and 2013, respectively. He is currently an Associate Professor with the Communication and Antenna Systems Division, Chalmers University of Technology. His current research interests include millimeter-wave planar antennas in general, gap waveguide technology, frequency-selective surfaces, microwave passive components, and the packaging techniques and integration of MMICs with the antennas.